

Modulo Sampling: Performance Guarantees in The Presence of Quantization

Neil Irwin Bernardo, *Member, IEEE*, Shaik Basheeruddin Shah, *Graduate Student Member, IEEE*,
and Yonina C. Eldar, *Fellow, IEEE*

Abstract—In this paper, we investigate the relationship between the dynamic range and quantization noise power in modulo analog-to-digital converters (ADCs). Two modulo ADC systems are considered: (1) a modulo ADC which outputs the folded samples and an additional 1-bit folding information signal, and (2) a modulo ADC without the 1-bit information. A recovery algorithm that unfolds the quantized modulo samples using the extra 1-bit folding information is analyzed. Using the dithered quantization framework, we show that an oversampling factor of $OF > 3$ and a quantizer resolution of $b > 3$ are sufficient conditions to unfold the modulo samples. When these conditions are met, we demonstrate that the mean squared error (MSE) performance of modulo ADC with an extra 1-bit folding information signal is better than that of a conventional ADC with the same number of bits used for amplitude quantization. Since folding information is typically not available in modulo ADCs, we also propose and analyze a recovery algorithm based on orthogonal matching pursuit (OMP) that does not require the 1-bit folding information. In this case, we prove that $OF > 3$ and $b > 3 + \log_2(\delta)$ for some $\delta > 1$ are sufficient conditions to unfold the modulo samples. For the two systems considered, we show that, with sufficient number of bits for amplitude quantization, the mean squared error (MSE) of a modulo ADC is $\mathcal{O}(\frac{1}{OF^3})$ whereas that of a conventional ADC is only $\mathcal{O}(\frac{1}{OF})$. We extend the analysis to the case of simultaneous acquisition of weak and strong signals occupying different frequency bands. Finally, numerical results are presented to validate the derived performance guarantees.

Index Terms—Modulo ADC, sampling, quantization, weak and strong signals.

I. INTRODUCTION

Most modern data acquisition systems are equipped with analog-to-digital converters (ADCs) to transform continuous-time observations to some format suitable for processing in the digital domain. Standard ADCs first sample the signal at equally-spaced time intervals and then the amplitudes of the samples are mapped to a finite set of discrete values by a quantizer [1]. The aim is to accurately represent the original analog signal in the digital domain. One critical consideration

Part of this work has been accepted for presentation at the IEEE International Symposium on Information Theory (ISIT) 2024.

N.I. Bernardo is with the Electrical and Electronics Engineering Institute, University of the Philippines Diliman, Quezon City 1101, Philippines (e-mail: neil.bernardo@eee.upd.edu.ph). S. B. Shah is with the Department of Electrical Engineering, Khalifa University, UAE (e-mail: shaik.shah@ku.ac.ae). Y. C. Eldar is with the Weizmann Institute of Science, Rehovot, Israel (e-mail: yonina.eldar@weizmann.ac.il).

This research was supported by the Tom and Mary Beck Center for Renewable Energy as part of the Institute for Environmental Sustainability (IES) at the Weizmann Institute of Science, by the European Research Council (ERC) under the European Union's Horizon 2020 research and innovation program (grant No. 101000967) and by the Israel Science Foundation (grant No. 536/22).

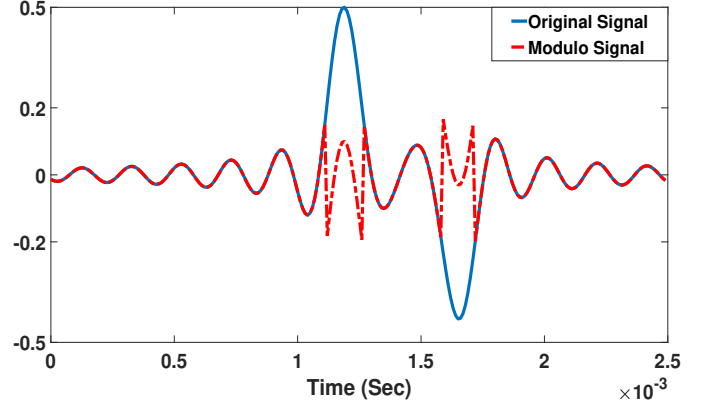


Fig. 1. A typical high DR input signal and the corresponding modulo signal with modulo operator threshold value equal to 0.2.

in an ADC design is ensuring that the dynamic range (DR) of the ADC exceeds that of the input signal, where DR refers to the difference between the smallest and largest values that can be represented. When the DR of the ADC falls short of capturing the full range of the input signal, clipping occurs [2]–[4]. This loss of information compromises the accuracy of the digital representation and impacts the reliability of subsequent data processing.

There exist different algorithms in the literature to address this challenge [5]–[8]. The recent unlimited sampling framework (USF) has emerged as a promising solution [9] to enable the acquisition of high DR signals using limited DR ADCs. In USF, the high DR input signal is pre-processed by a non-linear modulo operator. This modulo operator folds the input signal whenever it crosses some pre-defined modulo thresholds (see Fig. 1). Subsequently, the modulo signal serves as the input to the ADC. Following the ADC, a recovery algorithm is applied to unfold the output samples of the ADC. The integration of an ADC, a modulo pre-processing, and a recovery algorithm is referred to as a modulo ADC system.

One of the main focuses of existing works on modulo ADC is to develop a robust and computationally efficient recovery algorithm that operates close to the Nyquist rate. The existing literature presents diverse recovery algorithm strategies. These encompass higher-order-differences-based approach [9], prediction-based method [10], wavelet-based technique [11], Fourier-domain methodologies [12]–[15], and others. Among these methods, [13]–[16] are identified to be robust recovery algorithms approaching the Nyquist rate. Apart from recovery

algorithms, there are also efforts to advance the hardware implementation of modulo ADCs [12], [16]–[20]. Furthermore, USF has been studied extensively across various signal models, such as Finite-Rate-of-Innovation (FRI) signals [21], sparse signals [22]–[24], graph signals [25], and shift-invariant spaces [26], [27], among others.

Nevertheless, research addressing the impact of quantization on modulo ADCs is notably limited. In [9], the authors introduced a higher-order differences-based recovery algorithm for bandlimited (BL) signals that operates at approximately $2\pi e$ (≈ 17) times the Nyquist rate when there is no quantization. Theoretical guarantees for the higher-order show that this sufficient condition for the sampling rate becomes stricter in the presence of bounded noise [9]. To improve upon this, a prediction filter-based algorithm to unfold the modulo ADC output was proposed [10]. When the prediction filter is sufficiently long, this approach enables signal recovery at a rate close to the Nyquist rate. However, this recovery method fails in the presence of quantization noise. Recent work on USF radars [28] has investigated the impact of quantization on a modulo ADC if the input signal contains weak and strong components, however, this work uses higher-order differences to unfold the modulo samples. Signal-to-quantization noise ratio (SQNR) of modulo ADCs has been analyzed in [29] but the reconstruction method used relies on a separately encoded 2-bit reset signal.

This work aims to address this gap and provide a more comprehensive understanding of how modulo sampling and quantization interact, particularly in scenarios involving BL signals with diverse target strengths. Moreover, this study identifies suitable conditions for which a modulo ADC has better performance than a conventional ADC without modulo when the number of bits used for amplitude quantization are the same. The following are major contributions:

- 1) We analyze the recovery algorithm introduced in [16], which leverages the *bits distribution* mechanism to unfold the modulo ADC output. In [16], the algorithm allocates 1-bit from the total bit budget to detect modulo folding events. In contrast, this work assumes the full ADC resolution (b) is used for quantization, with an additional 1-bit folding information explicitly provided by the modulo ADC. Within a dithered quantization framework, we evaluate the reconstruction performance of this approach. We establish sufficient conditions on the oversampling factor (OF) and b to ensure that the modulo ADC offers superior quantization noise suppression compared to conventional ADCs without the modulo operator. Specifically, we prove that $\text{OF} > 3$ and $b > 3$ are enough for the modulo ADC to achieve lower mean squared error (MSE) than conventional ADCs.
- 2) Since the 1-bit folding information is generally unavailable in the modulo ADC, we propose and examine an orthogonal matching pursuit (OMP)-based recovery algorithm to unfold the modulo ADC output. Our analysis demonstrates that ensuring $\text{OF} > 3$ and $b > 3 + \log_2(\delta)$, where $\delta > 1$ is some constant, is sufficient for achieving superior quantization noise suppression in modulo ADCs over conventional ADCs. Additionally,

we present a case study that analyzes a BL signal having both weak and strong components occupying different frequency bands and demonstrate that a modulo ADC outperforms a conventional ADC in capturing the strong and weak signal components simultaneously.

- 3) We show that for the aforementioned settings, the MSE of the modulo ADC is on the order of $\mathcal{O}\left(\frac{1}{\text{OF}^3}\right)$, while that of a standard ADC is on the order of $\mathcal{O}\left(\frac{1}{\text{OF}}\right)$. This underscores the importance of oversampling in modulo ADC in retrieving the original signal from quantized modulo observations. Finally, we validate the proposed theory with numerical simulations.

The paper is organized as follows: The two modulo ADC system models considered in the study and our proposed recovery methods are described in Section II. Theoretical MSE performance guarantees for the recovery algorithms are established in Section III. Then, we specialize our derived performance guarantees to the case of simultaneous acquisition of weak and strong signals in Section IV. Numerical results are provided in Section V to validate our proposed theory. Finally, we summarize the work in Section VI.

Notation: The following notations are used throughout the paper. We denote the set of real numbers, integers, and natural numbers as \mathbb{R} , \mathbb{Z} , and \mathbb{N} , respectively. The space of square-integrable functions on \mathbb{R} is represented by $L^2(\mathbb{R})$, and $\mathbb{E}[\cdot]$ denotes the expectation operator. We use bold lowercase letters to represent vectors, and bold capital letters to denote matrices. The ℓ_p -norm of a vector \mathbf{z} is denoted as $\|\mathbf{z}\|_p$, with a similar notation extending to ℓ_p -norms of functions. When referring to discrete-time signals, we employ the notation $z[n]$ to signify $z(nT_s)$, assuming the sampling period T_s is evident from the context. For a discrete-time signal $x[n]$, the first-order difference operator is defined as $\Delta x[n] = x[n] - x[n-1]$, under the assumption that $x[-1] = 0$. To describe the growth rate of a quantity concerning some parameter, we employ standard asymptotic notation, such as $\mathcal{O}(\cdot)$. The cumulative sum operation applied to a vector $\mathbf{x} \in \mathbb{R}^{N \times 1}$ yields a vector $\mathbf{y} \in \mathbb{R}^{N \times 1}$, where the k^{th} element of \mathbf{y} is given by $y_k = \sum_{i=1}^k x_i$. The pseudo-inverse of a matrix $\mathbf{A} \in \mathbb{R}^{m \times n}$, where $n \gg m$, is denoted by \mathbf{A}^\dagger , and defined as $\mathbf{A}^\dagger = (\mathbf{A}^T \mathbf{A})^{-1} \mathbf{A}^T$.

II. MODULO ADC PROBLEM SETUP AND PROPOSED RECOVERY METHODS

In this section, we describe the two modulo ADC system models to be analyzed in this work: (1) a modulo ADC that generates the quantized folded samples and an extra 1-bit folding information, and (2) a modulo ADC without the extra 1-bit folding information. We present the proposed recovery algorithms for these two system models.

A. Modulo ADC System With Extra 1-Bit Folding Information

We consider the modulo ADC system shown in Fig. 2a. The input $f(t) \in L^1(\mathbb{R})$ is a bandlimited signal with frequency support $[-\frac{\omega_m}{2}, +\frac{\omega_m}{2}]$. The input signal is fed to a non-linear modulo sampling block, denoted $\mathcal{M}_{\lambda'}(\cdot)$, to produce

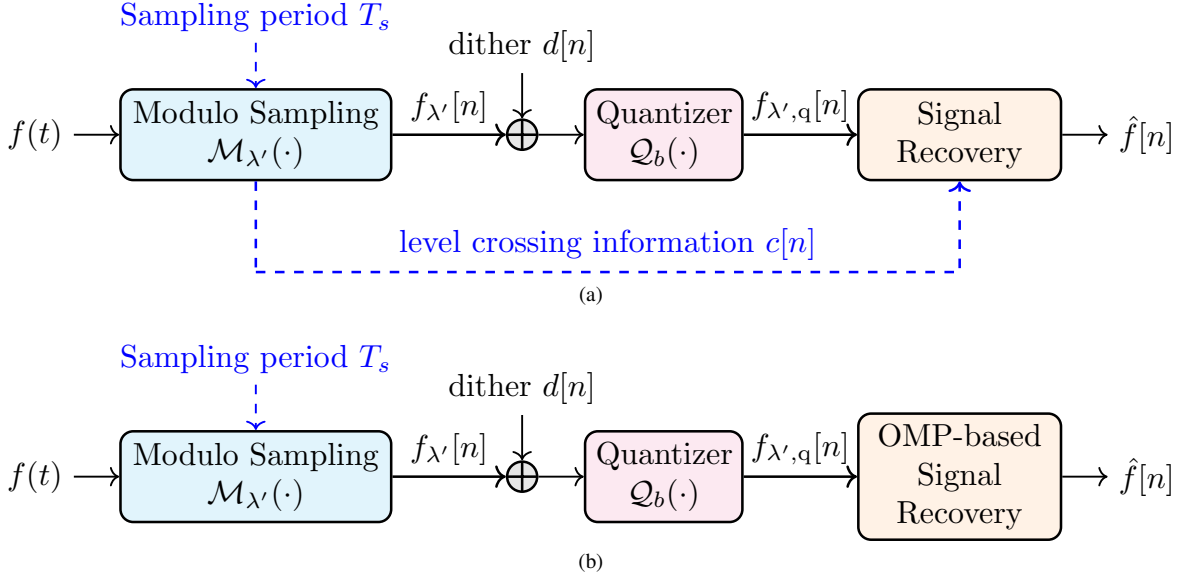


Fig. 2. Schematic diagram of (a) a modulo sampling system with dithered quantization. A 1-bit folding information signal is also generated by $\mathcal{M}_{\lambda'}(\cdot)$ to aid in signal reconstruction. In (b), the extra 1-bit folding information signal is removed.

the discrete-time modulo observations $f_{\lambda'}[n]$, $n \in \mathbb{Z}$. Mathematically,

$$\begin{aligned} f_{\lambda'}[n] &= \mathcal{M}_{\lambda'}(f(t)) \\ &= [(f(nT_s) + \lambda') \bmod 2\lambda'] - \lambda', \end{aligned} \quad (1)$$

where $\lambda' \in (0, \|f(t)\|_{\infty})$ is the modulo operator threshold. The range of λ' is chosen to exclude the trivial case that the input signal amplitude is within the linear region of the modulo. The sampling rate is $\omega_s = \frac{2\pi}{T_s} = \text{OF} \times \omega_m$, where $\text{OF} > 1$. We will also use $\rho = \frac{1}{\text{OF}}$ in the analysis.

The folded samples are fed to a b -bit scalar quantizer $\mathcal{Q}_b(\cdot)$ with dynamic range $[-\lambda, +\lambda]$. The nonlinearity of the quantization process makes it difficult to analyze the impact of quantization in modulo sampling. To this end, a dither signal $d[n]$ is added to $f_{\lambda'}[n]$ prior to quantization. An independent and identically-distributed (i.i.d.) triangle noise sequence with amplitude support $(-\frac{2\lambda}{2^b}, +\frac{2\lambda}{2^b})$ is used for the dither signal $d[n]$. The rationale for incorporating a triangle dither in the system model is twofold. First, the modulo operation can be set so that $f_{\lambda'}[n] + d[n]$ will not overload the quantizer. This, together with the properties of triangle dither, guarantees that Shuchman conditions [30] are satisfied, which allows the first-order and second-order statistics of the quantization noise to be derived from the system parameters. Second, the sequences $\epsilon[n]$ and $f_{\lambda'}[n]$ become uncorrelated and the conditional second-order moment of $\epsilon[n]$ becomes independent of $f_{\lambda'}[n]$, i.e., $\mathbb{E}[\epsilon^2[n]|f_{\lambda'}[n]] = \mathbb{E}[\epsilon^2[n]]$.

Each quantization bin has a width of $\frac{2\lambda}{2^b}$. To prevent the signal from overloading the quantizer, we set the modulo threshold to be $\lambda' = \frac{(2^b - 2)\lambda}{2^b}$. The quantizer output can then be written as

$$\begin{aligned} f_{\lambda',q}[n] &= \mathcal{Q}_b(f_{\lambda'}[n] + d[n]) \\ &= f[n] + z[n] + \epsilon[n], \end{aligned} \quad (2)$$

where $z[n] \in 2\lambda'\mathbb{Z}$ is the residual samples due to the folding operation of $\mathcal{M}_{\lambda'}(\cdot)$ and $\epsilon[n] = \mathcal{Q}_b(f_{\lambda'}[n] + d[n]) - f_{\lambda'}[n]$ is the quantization noise sequence. With triangle dither, the quantization noise is a white process with noise power [31]

$$\mathbb{E}[\epsilon^2[n]] = \frac{1}{4} \left(\frac{2\lambda}{2^b} \right)^2 = \frac{\lambda^2}{2^{2b}}. \quad (3)$$

We will use the statistical properties of $\epsilon[n]$ to establish MSE performance guarantees in Section III. However, note that the inclusion of a triangular dither signal is mainly for analytical tractability. We show in Section V that our proposed recovery methods work even without the dither signal.

In addition to $f_{\lambda'}[n]$, the modulo sampling block also generates a 1-bit discrete-time binary signal $c[n]$ which contains information about the $(2\mathbb{Z} + 1)\lambda'$ level crossings in $f(t)$. More precisely, $c[n] = 1$ whenever the input signal crosses the level $(2\mathbb{Z} + 1)\lambda'$ within the time interval $(nT_s, (n+1)T_s)$ while $c[n] = 0$ otherwise. The set of indices n where $c[n] = 1$ is denoted as \mathcal{S} . There are several ways to generate this 1-bit folding information. One approach is explored in [16], which only incurs one additional OR gate to the setup. This penalty is fixed regardless of b . From a power efficiency viewpoint, this additional OR gate has minimal impact on the power consumption of the modulo ADC.

B. Signal Recovery for Modulo ADC With 1-Bit Folding Information

The signal recovery block utilizes the information about \mathcal{S} to recover the modulo residue $z[n]$. The underlying reconstruction algorithm is based on [16], [32]. Since $f(t) \in L^1(\mathbb{R})$, $\lim_{|t| \rightarrow \infty} f(t) = 0$ by the Riemann-Lebesgue lemma [33, Chapter 12]. Consequently, for any $\lambda' > 0$, there exist integers n_0 and n_1 ($n_0 < n_1$) such that $|f(nT_s)| < \lambda$ for all $n_0 > n$ and $n_1 < n$. the residual samples $z[n]$ can be treated as a

finite-duration discrete-time signal of length $N = n_1 - n_0 + 1$. We define a $K \times 1$ vector $\mathbf{y} = [y_0, \dots, y_{K-1}]^T$, where

$$\begin{aligned} y_k &= \frac{1}{\sqrt{N}} \sum_{n=n_0}^{n_1} [f_{\lambda',q}[n] - f_{\lambda',q}[n-1]] e^{-j\frac{2\pi nk}{N}} \\ &= \frac{1}{\sqrt{N}} \sum_{n=n_0}^{n_1} [\Delta z[n] + \Delta \epsilon[n]] e^{-j\frac{2\pi nk}{N}} \\ &= \frac{1}{\sqrt{N}} \left(\sum_{n \in \mathcal{S}} [\Delta z[n] + \Delta \epsilon[n]] e^{-j\frac{2\pi nk}{N}} \right. \\ &\quad \left. + \sum_{n=n_0, n \notin \mathcal{S}}^{n_1} \Delta \epsilon[n] e^{-j\frac{2\pi nk}{N}} \right). \end{aligned}$$

Here, $\frac{2\pi k}{N}$ is one of the $K < N$ discrete frequencies inside $(\rho\pi, 2\pi - \rho\pi)$. The second line follows from the fact that the signal $f[n]$ is outside $(\rho\pi, 2\pi - \rho\pi)$. The third line follows from putting all terms with $n \in \mathcal{S}$ in the first summation and putting the remainder in the second summation. Notice that the information we want to extract (residual samples) is only contained in the first summation. We vectorize $\Delta z[n]$ by forming the vector $\Delta \mathbf{z} = [\Delta z[n_0], \dots, \Delta z[n_1]]^T$. We also define the $|\mathcal{S}| \times 1$ vector $\Delta \mathbf{z}_{\mathcal{S}}$ which contains the nonzero elements of $\Delta \mathbf{z}$ at indices found in the set \mathcal{S} while the $(N - |\mathcal{S}|) \times 1$ vector $\Delta \mathbf{z}_{\mathcal{S}^c}$ is an all-zero vector.

Let $\mathbf{V} \in \mathbb{R}^{K \times N}$ with elements $\mathbf{V}_{k,n} = e^{-j\frac{2\pi nk}{N}}$, where $\frac{2\pi k}{N}$ is the k -th discrete frequency in $(\rho\pi, 2\pi - \rho\pi)$. The matrix $\mathbf{V}_{\mathcal{S}} \in \mathbb{R}^{K \times |\mathcal{S}|}$ contains the $|\mathcal{S}|$ columns of \mathbf{V} corresponding to the indices in \mathcal{S} . An estimate of the non-zero elements of the first-order difference vector, denoted $\Delta \hat{\mathbf{z}}_{\mathcal{S}}$, can be formed by

$$\Delta \hat{\mathbf{z}}_{\mathcal{S}} = \mathbf{V}_{\mathcal{S}}^{\dagger} \mathbf{y}. \quad (4)$$

The estimate of the vector $\Delta \mathbf{z}$, denoted $\Delta \hat{\mathbf{z}}$, is obtained by combining $\Delta \hat{\mathbf{z}}_{\mathcal{S}}$ and $\Delta \hat{\mathbf{z}}_{\mathcal{S}^c}$. The elements of $\Delta \hat{\mathbf{z}}$ are rounded to the nearest $2\lambda' \mathbb{Z}$. Then a cumulative sum is applied to the resulting vector to obtain the estimate of the modulo residue, denoted $\hat{\mathbf{z}} = (\Delta \hat{\mathbf{z}})_{\Sigma}$. Let $\hat{z}[n]$ be the discrete-time representation of the vector $\hat{\mathbf{z}}$. We subtract $\hat{z}[n]$ from $f_{\lambda',q}[n]$ to remove the modulo residue from the quantized modulo observations. Finally, we apply an ideal digital lowpass filter, $\text{LPF}\{\cdot\}$, with passband region $(-\frac{\omega_m}{2}, +\frac{\omega_m}{2})$. The recovered signal can be written as

$$\begin{aligned} \hat{f}[n] &= \text{LPF}\{f_{\lambda',q}[n] - \hat{z}[n]\} \\ &= f[n] + \text{LPF}\{z[n] - \hat{z}[n]\} + \text{LPF}\{\epsilon[n]\}. \end{aligned} \quad (5)$$

Hence, the recovered signal is composed of the desired samples, filtered modulo residue estimation error, and filtered quantization noise.

C. Modulo ADC Without 1-Bit Folding Information

In a typical modulo ADC system, the 1-bit folding information signal may not be available for the reconstruction method. Thus, it is also of interest to develop a recovery algorithm for the modulo ADC shown in Fig. 2b. Since the 1-bit folding information tells the exact locations of nonzero elements of Δz , one approach to facilitate the signal reconstruction is to

perform support recovery of $\Delta z[n]$ and then run the signal reconstruction algorithm described in Section II-B, with $c[n]$ being replaced by $\hat{c}[n]$, the recovered support of $\Delta z[n]$. Note that $\Delta z[n]$ is a sparse signal [15]. Thus, we can utilize existing support recovery algorithms for sparse signals and their corresponding theoretical guarantees.

For the support recovery of $\Delta z[n]$, we consider the greedy *orthogonal matching pursuit* (OMP) algorithm [34], [35], which uses a stopping rule based on the ℓ_{∞} -norm of the bounded noise [36]. More precisely, $\hat{c}[n]$ is obtained as follows:

- 1) Initialize the index set $\mathcal{I} = \emptyset$, the residue $\mathbf{r}_0 = \mathbf{y}$, the estimator $\mathbf{x}_0 = \mathbf{0}$, and the iteration counter $t = 1$.
- 2) At time t , select a column from \mathbf{V} that is most correlated with the current residue \mathbf{r}_{t-1} , i.e.,

$$n_t = \arg \max_n |\langle \mathbf{v}_n, \mathbf{r}_{t-1} \rangle|,$$

where \mathbf{v}_n is the n -th column of \mathbf{V} . The index n_t is added to the index set \mathcal{I} .

- 3) Calculate the new estimator \mathbf{x}_t by projecting \mathbf{y} onto the space spanned by $\mathbf{V}_{\mathcal{I}}$, i.e., $\mathbf{x}_t = \mathbf{V}_{\mathcal{I}}^{\dagger} \mathbf{y}$. Update residual $\mathbf{r}_t = \mathbf{y} - \mathbf{V}_{\mathcal{I}} \mathbf{x}_t$.
- 4) Stop if $\|\mathbf{V}_{\mathcal{I}}^H \mathbf{r}_t\|_{\infty} \leq \eta \frac{6\lambda'}{2^{b-2}}$, where $\eta = \|\mathbf{V}^H \mathbf{V}\|_{\infty}$ and set

$$\hat{c}[n] = \begin{cases} 1, & n \in \mathcal{I} \\ 0, & n \notin \mathcal{I} \end{cases}.$$

Otherwise, set iteration counter to $t = t + 1$ and return to Step 2.

The stopping criterion in step 4 is used so that the residue is less than the ℓ_{∞} -norm of $\Delta \epsilon$. Once $c[n]$ has been estimated, we can apply the recovery algorithm in Section II-B accordingly.

Our aim is to derive MSE performance guarantees for the two modulo ADC systems presented when the proposed recovery algorithms are used. Additionally, we also want to identify suitable settings for which the modulo ADC has superior performance compared to a conventional ADC without modulo. Furthermore, we extend this analysis to a critical scenario involving the simultaneous acquisition of weak and strong signals occupying different frequency bands in a BL signal. The following sections present these performance guarantees in detail.

III. RECOVERY GUARANTEES

We quantify the recovery performance of the modulo ADC using the MSE criterion. In general, the MSE can be expressed as a sum of two errors: (1) a truncation error due to neglecting the signal values outside $n < n_0$ and $n > n_1$, and (2) a reconstruction error due to the modulo residue estimation error and finite quantization. In this paper, we focus on the latter since we can set n_0 and n_1 so that $f[n] \approx 0$ outside the discrete-time interval $[n_0, n_1]$. Consequently, the truncation error can be set to a negligible value. Henceforth, we refer to the reconstruction error whenever MSE is mentioned.

A. MSE guarantee for Modulo ADC With 1-Bit Folding Information

We first focus on the MSE performance guarantee for the modulo ADC with 1-bit folding information. One important property to ensure correct signal unfolding is to show that \mathbf{V}_{S_i} is a full column rank matrix. With \mathbf{V}_S being full column rank, there is a unique solution to the equation $\mathbf{y} = \mathbf{V}_S \cdot \Delta \mathbf{z}_S$. The following key lemma shows that an OF value greater than three is a sufficient (but not necessary) condition to make \mathbf{V}_S a full column rank matrix.

Lemma 1. *Suppose $\text{OF} > 3$. Then \mathbf{V}_S has full column rank if the modulo threshold $\lambda' \geq \frac{\|f(t)\|_\infty}{\text{OF}-2}$.*

Proof. See Appendix A. \square

For a given $f(t)$, it actually suffices that $\text{OF} \geq \frac{N}{N-|\mathcal{S}|}$ to make \mathbf{V}_S full column rank. However, such condition depends on the specific $f(t)$. By using the upper bound on $|\mathcal{S}|$ established in [15], we eliminate the dependence on the specific $f(t)$ and find an oversampling factor requirement that holds for any $f(t)$. However, the bound on $|\mathcal{S}|$ is not tight in general as demonstrated in [15, Table 1].

We are now ready to state the main result of this paper. The following theorem gives the exact MSE of the modulo ADC system in Fig. 2a when $b > 3$, $\text{OF} > 3$, and λ' is set to be $\frac{\|f(t)\|_\infty}{\text{OF}-2}$.

Theorem 1. *Suppose $b > 3$ and $\text{OF} > 3$. Then the MSE of the reconstruction procedure for the modulo ADC with extra 1-bit folding information is*

$$\mathbb{E}[(f[n] - \hat{f}[n])^2] = \frac{1}{\text{OF}(2^b - 2)^2} \cdot \left(\frac{\|f(t)\|_\infty}{\text{OF} - 2} \right)^2 \quad (6)$$

if we set $\lambda' = \frac{\|f(t)\|_\infty}{\text{OF}-2}$.

Proof. See Appendix B. \square

The intuition of the proof is to set a sufficiently large number of quantization bits such that the induced quantization noise is not strong enough to put the recovered first-order difference of the residue outside $(2\lambda'p - \lambda', 2\lambda'p + \lambda')$ if $z[n] = 2\lambda'p$ for some $p \in \mathbb{Z}$. In this case, the rounding operation on the elements of $\Delta \hat{z}$ is perfect, i.e. $\hat{z}[n] = z[n]$, and the only impairment in $\hat{f}[n]$ is the (lowpass-filtered) quantization noise.

We now compare our derived MSE for the modulo ADC in Fig. 2a with that of the conventional ADC without modulo sampling. To get the behavioral model of a conventional ADC, we simply replace $\mathcal{M}_{\lambda'}(\cdot)$ in Fig. 2a with a regular sampler with sampling period T_s and then remove $c[n]$. To obtain analytical results for conventional ADCs, we also use the non-subtractive dithered quantization framework. With triangle dither $d[n] \in (-\frac{2\lambda}{2^b}, +\frac{2\lambda}{2^b}]$, we must set λ of the conventional ADC as $\lambda = \frac{2^b}{2^b-2} \|f(t)\|_\infty$ to prevent overloading. Consequently, the quantization noise is white and has a mean squared value of $\mathbb{E}[\epsilon^2[n]] = \frac{\lambda^2}{2^{2b}}$. With an oversampling factor of OF, the desired signal occupies only $\frac{1}{\text{OF}}$ of $(-\pi, +\pi)$ band. A lowpass filter with passband region $(-\rho\pi, +\rho\pi)$ can be used to filter out the quantization noise in the out-of-band region.

Thus, the MSE is solely attributed to the filtered quantization noise and can be expressed as

$$\text{MSE}^{(\text{no-modulo})} = \frac{1}{\text{OF}(2^b - 2)^2} \cdot \|f(t)\|_\infty^2. \quad (7)$$

By comparing (7) with the result in Theorem 1, we see that, for the same number of bits for amplitude quantization, the quantization noise power of the modulo ADC is strictly lower than that of the conventional ADC when $\text{OF} > 3$ and $b > 3$. In fact, it can be observed that $\text{MSE}^{(\text{no-modulo})} = \mathcal{O}\left(\frac{1}{\text{OF}}\right)$ whereas $\text{MSE}^{(\text{with-modulo})} = \mathcal{O}\left(\frac{1}{\text{OF}^3}\right)$. This sheds light on the advantage of modulo ADCs over conventional ADCs.

We also compare our results with other theoretical guarantees derived for modulo sampling. The impact of bounded noise (e.g., quantization) has been analyzed in [9, Theorem 3] when the recovery algorithm is based on higher-order differences (HOD). Their analysis guarantees the recovery of the samples up to an unknown additive constant, i.e., $\hat{f}^{(\text{HOD})}[n] = f[n] + \epsilon[n] + 2\lambda'p$ for some unknown $p \in \mathbb{Z}$. By ignoring the unknown additive constant and applying an appropriate noise filtering, the MSE of the HoD should be identical to that of our proposed recovery algorithm. However, under this bounded noise setting, the sufficient condition to achieve this performance guarantee is that the sampling rate should be at least $2^\alpha \pi e$ times the Nyquist rate, where $\alpha \in \mathbb{N}$ is a noise-dependent parameter. In contrast, our analytical result does not have an unknown additive constant and the exact MSE can be derived at any $\text{OF} > 3$.

B. MSE Guarantee for Modulo ADC Without 1-Bit Folding Information

We now consider the modulo ADC system in Fig. 2b and establish a recovery performance guarantee for the proposed algorithm in Section II-C. Since the proposed algorithm is based on OMP, we restate a theorem from [37] which identifies a sufficient condition on the minimum amplitude of the noisy sparse signal to ensure perfect support recovery.

Theorem 2. *(from [37, Theorem 2]) Consider the observation signal $\mathbf{y} = \mathbf{A}\mathbf{x} + \mathbf{e}$. Suppose that $\|\mathbf{A}^H \mathbf{e}\| \leq \epsilon_0$ and matrix \mathbf{A} satisfies*

$$\delta_{L+1} < \frac{1}{\sqrt{L} + 1}, \quad (8)$$

where δ_L is the restricted isometry property (RIP) constant order L of matrix \mathbf{A} . Then, the OMP with stopping rule $\|\mathbf{A}^H \mathbf{e}\| \leq \epsilon_0$ will exactly recover the support Ω of an L -sparse signal \mathbf{x} from the observation signal \mathbf{y} if the minimum magnitude of nonzero elements of \mathbf{x} satisfies

$$\min_{i \in \Omega} |\mathbf{x}_i| > \frac{(\sqrt{1 + \delta_{L+1}} + 1) \sqrt{L} \epsilon_0}{1 - (\sqrt{L} + 1) \delta_{L+1}}. \quad (9)$$

Using Theorem 2, we identify a sufficient condition on the quantizer resolution b to ensure that OMP will produce $\hat{c}[n] = c[n]$. With perfect $\hat{c}[n]$, we can apply Theorem 1 to obtain recovery guarantees for the proposed algorithm in Section II-C.

Theorem 3. Set $\lambda' = \frac{\|f(t)\|_\infty}{\text{OF}-2}$ and let

$$L_0 = 4 \left\lfloor \frac{N}{2\text{OF}} \right\rfloor + 4 \left\lfloor \frac{N}{2\text{OF}} \right\rfloor \cdot \left\lfloor \frac{\text{OF} - 3}{2} \right\rfloor. \quad (10)$$

Suppose matrix \mathbf{V} satisfies the RIP of order L_0 with an RIP constant denoted as δ_L and that $\delta_{L_0} < \frac{1}{\sqrt{L_0+1}}$. Let $\eta = \|\mathbf{V}^H \mathbf{V}\|_\infty$. If $\text{OF} > 3$ and

$$b > 3 + \log_2 \left\{ \frac{3\eta \cdot \frac{(\sqrt{1+\delta_{L_0+1}}+1)\sqrt{L_0}}{1-(\sqrt{L_0+1})\delta_{L_0+1}} + 1}{4} \right\}, \quad (11)$$

then $c[n]$ can be perfectly recovered using OMP with stopping rule $\|\mathbf{V}^H \mathbf{r}_t\|_\infty \leq \eta \frac{6\lambda'}{2^b-2}$. The MSE of the OMP-based reconstruction procedure for the modulo ADC system without the 1-bit folding information signal is

$$\text{MSE} = \frac{1}{\text{OF}(2^b-2)^2} \cdot \left(\frac{\|f(t)\|_\infty}{\text{OF}-2} \right)^2. \quad (12)$$

Proof. See Appendix C. \square

The main difference between Theorem 3 and Theorem 1 is the quantization bit requirement needed to obtain the performance guarantees. The argument inside the logarithm in (11) can be shown to be greater than 1. Thus, the sufficient condition on the quantization bits becomes more stringent in the absence of 1-bit folding information $c[n]$. One major limitation of the bound is that it depends on the RIP constant δ_{L_0+1} . Testing whether a sensing matrix satisfies RIP is an NP-hard problem [38]. We also note that a different sparse recovery algorithm other than OMP can be used to recover $c[n]$. For instance, the LASSO-B²R² [15] uses the iterative soft-thresholding algorithm (ISTA) for sparse recovery.

IV. CASE STUDY: SIMULTANEOUS ACQUISITION OF WEAK AND STRONG SIGNALS

We now investigate the case of simultaneous acquisition of weak and strong signals that occupy different frequency bands, as shown in Figure 3. The modulo ADC block is based on Fig. 2a and the digital channelizer implements a digital bandpass filter that can be tuned to the desired channel. This case is particularly interesting due to the conflicting requirements to capture the two signals. Setting the dynamic range too high to capture the strong signal can bury the weak signal in quantization noise. Meanwhile, setting the dynamic range too low could distort the strong signal. A recent work on USF [28] considers the issue of weak and strong components. However, their mathematical formulation of the problem only assumes a two-tone input signal with different amplitudes. Moreover, performance improvements of modulo ADC over conventional ADCs are only presented via numerical simulations. To the best of our knowledge, a theoretical analysis of the simultaneous acquisition of weak and strong signals using modulo ADC has not been conducted. Our goal in this section is to provide a more general mathematical formulation of the problem and a rigorous analysis to justify the advantage of modulo ADC over conventional ADCs in this case.

The bandlimited input signal $f(t)$ is modeled as a two-component signal of the form

$$f(t) = \alpha_1 f_1(t) + \alpha_2 f_2(t), \quad (13)$$

where $f_1(t)$ and $f_2(t)$ are bandpass signals. Denote \mathcal{F}_1 and \mathcal{F}_2 the frequency supports of $f_1(t)$ and $f_2(t)$, respectively. We impose $\mathcal{F}_1 \cap \mathcal{F}_2 = \emptyset$ and $\mathcal{F}_1 \cup \mathcal{F}_2 \in [-\omega_m/2, +\omega_m/2]$, i.e., $f_1(t)$ and $f_2(t)$ have different frequency supports and they both reside inside $[-\omega_m/2, +\omega_m/2]$. The bandwidths of $f_1(t)$ and $f_2(t)$ are ω_1 and ω_2 , respectively. Without loss of generality, we set $\|f_1(t)\|_2^2 = 1$ and $\|f_2(t)\|_2^2 = 1$. The simultaneous acquisition of strong and weak signals is modeled by setting $\alpha_1 \gg \alpha_2$. Since $f(t)$ is a bandlimited signal with energy $\alpha_1^2 + \alpha_2^2$, we have $\|f(t)\|_\infty \leq \sqrt{\frac{\omega_m(\alpha_1^2 + \alpha_2^2)}{\pi}}$ by [39].

The modulo ADC system in Fig. 2a is adopted in this case study. The reconstruction procedure described in Section II-B is modified to facilitate recovery of the individual components. Define $\text{BPF}_i\{\cdot\}$ to be an ideal digital bandpass filter with bandwidth ω_i and passband region \mathcal{F}_i . After estimating $\hat{z}[n]$, we apply the filter $\text{BPF}_i\{\cdot\}$ to $f_{\lambda',q}[n] - \hat{z}[n]$ to recover the i -th signal. Effectively, the recovered signal is

$$\hat{f}_i[n] = \alpha_i f_i[n] + \text{BPF}_i\{z[n] - \hat{z}[n]\} + \text{BPF}_i\{\epsilon[n]\}.$$

Performance of the modified reconstruction procedure is measured using the normalized MSE (NMSE) incurred when recovering the i -th signal, which can be expressed as

$$\begin{aligned} \text{NMSE}_i &= \frac{\mathbb{E}[(\alpha_i f_i[n] - \hat{f}_i[n])^2]}{\alpha_i^2} \\ &= \frac{1}{\alpha_i^2} \mathbb{E}[(\text{BPF}_i\{z[n] - \hat{z}[n]\} + \text{BPF}_i\{\epsilon[n]\})^2]. \end{aligned}$$

At this point, one might consider separating the two signal components in the analog domain using a tunable bandpass filter. This approach suppresses the strong signal component before it reaches the ADC. However, such an approach is costly to implement in analog. Moreover, analog filters exhibit severe group delay near the band edges, causing signal distortion. In contrast, a tunable digital filter can be implemented by varying the filter coefficients in the registers. Furthermore, achieving a linear phase response is straightforward in digital filters by imposing symmetry on the filter coefficients [40].

The following corollary of Theorem 1 provides an upper bound for NMSE_i when $b > 3$ and $\text{OF} > 3$.

Corollary 1. Suppose $b > 3$ and $\text{OF} > 3$. Then the NMSE incurred when recovering the i -th component under the modified reconstruction procedure is

$$\text{NMSE}_i \leq \frac{\omega_i}{\alpha_i^2} \cdot \frac{2}{\text{OF}(2^b-2)^2} \cdot \left(\frac{1}{\text{OF}-2} \right)^2 \cdot \left(\frac{\alpha_1^2 + \alpha_2^2}{\pi} \right) \quad (14)$$

Proof. See Appendix D. \square

Corollary 1 states that NMSE_i decreases linearly with $\frac{\alpha_i^2}{\omega_i}$. This indicates that, in addition to signal power, bandwidth plays a crucial role in determining recovery performance.

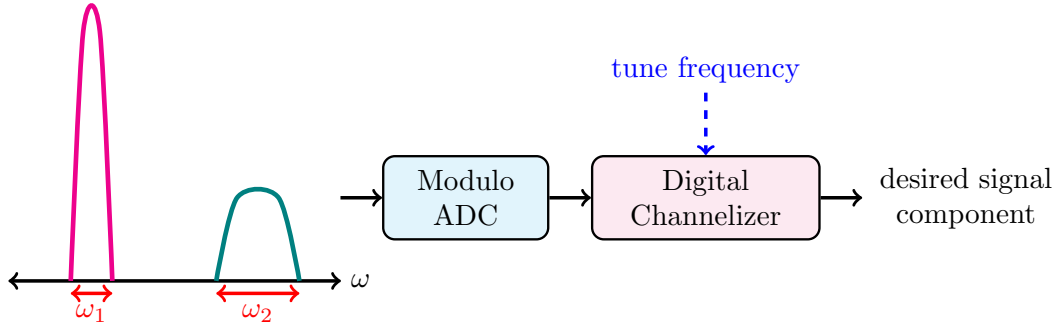


Fig. 3. Illustration of simultaneous acquisition of weak and strong signal components using a modulo ADC. The digital channelizer can be tuned to select between the weak and strong components.

Furthermore, if we use conventional ADCs with $b > 3$ and $\text{OF} > 3$, we would get

$$\text{NMSE}_i^{(\text{no-modulo})} \leq \frac{\omega_i}{\alpha_i^2} \cdot \frac{2}{\text{OF}(2^b - 2)^2} \cdot \frac{(\alpha_1^2 + \alpha_2^2)}{\pi}. \quad (15)$$

The RHS of (15) is strictly larger than the bound given in Corollary 1. In addition, the $\text{NMSE}_i = \mathcal{O}\left(\frac{1}{\text{OF}^3}\right)$ for modulo ADC whereas $\text{NMSE}_i = \mathcal{O}\left(\frac{1}{\text{OF}}\right)$ for conventional ADC. This demonstrates the advantage of using modulo ADC over a conventional ADC for the simultaneous acquisition of weak and strong signals. While the analysis above considered only two signal components with different frequency supports, it can be extended to $K > 2$ signal components as long as they all have disjoint frequency supports. The NMSE of the k -th signal component will still be inversely proportional to $\frac{\alpha_k^2}{\omega_k}$, where α_k^2 and ω_k are the energy and angular frequency of the k -th signal component, respectively.

V. NUMERICAL RESULTS

In this section, we perform the following simulations to substantiate the proposed theory. The aim is to show that the modulo ADC surpasses the conventional ADC lacking the modulo operator in terms of quantization noise reduction. This is accomplished by examining the variation of quantization noise power, represented by the MSE, as the OF value varies.

Simulation-1: In this simulation, we consider the modulo ADC system with side information as depicted in Fig. 2a. Specifically, we analyze the variation of MSE, as described in Theorem 1 and (7), as the OF value varies.

Consider the input signal

$$f(t) = \sum_{i=1}^5 A_i (\text{sinc}(f_m(t - \tau_i)))^2, \quad 0 \leq t < T, \quad (16)$$

where $\text{sinc}(x) = \frac{\sin(\pi x)}{\pi x}$ for any $x \neq 0$. This signal entails a maximal frequency component of $f_m = 50$ Hz, and a temporal duration of $T = 1$ second. Random coefficients A_i are drawn uniformly from the range $[-1, 1]$. While time offsets τ_i are chosen randomly within the interval $(\frac{T}{4}, \frac{3T}{4})$, this is to ensure that the residual signal remains zero outside the interval $(0, T)$. Additionally, we normalize $f(t)$ such that $\|f(t)\|_\infty = 1$. Consequently, the modulo threshold is $\lambda' = \frac{1}{\text{OF}^{-2}}$. We consider the number of bits b equal to 4 and sweep the OF

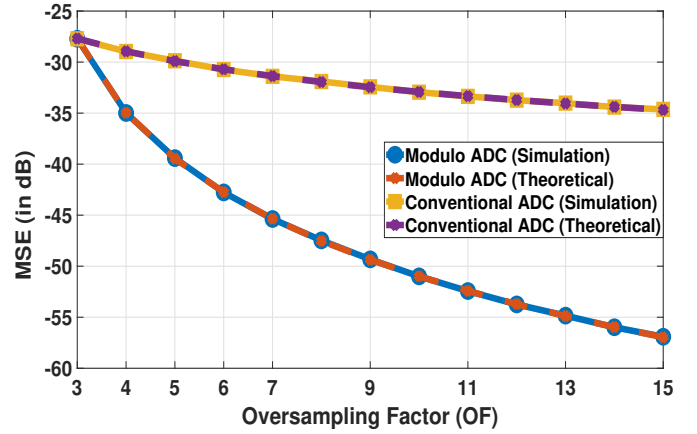


Fig. 4. Numerical and theoretical MSE results vs. OF for both modulo ADC with extra 1-bit information and conventional ADC.

values from 3 to 15. The dither signal and uniform quantizer are configured according to these parameters. For each OF value, we compute the MSE between true samples, $f[n]$, and the estimated samples, $\hat{f}[n]$. The experiment is repeated for 20000 i.i.d. noise realizations and the errors are averaged over all realizations.

Fig. 4 depicts the results obtained with this setting. It is evident from the figure that the MSE of the modulo ADC decays much faster than that of the conventional ADC without the modulo operator. Therefore, from Fig. 4, we conclude that the quantization noise suppression of modulo ADC is better than that of conventional ADC. Moreover, it is worth noting that for $\text{OF} = 3$, $\lambda' = \|f(t)\|_\infty$, and the MSE values of both modulo ADC and conventional ADC are equal. Fig. 4 also depicts theoretical MSE values obtained using Theorem 1 and (7). Note that both theoretical predictions match the simulated results. This justifies the accuracy of our analytical results and further emphasizes the fact that the MSE decays with the order of $\mathcal{O}\left(\frac{1}{\text{OF}^3}\right)$ and $\mathcal{O}\left(\frac{1}{\text{OF}}\right)$ for modulo ADC and conventional ADC, respectively. As a final remark, the use of the extra 1-bit side information in Fig. 2a only incurs one additional OR gate to the setup [16]. This penalty is fixed regardless of b . From a power efficiency viewpoint, this additional OR gate has minimal impact on the power consumption of modulo ADC.

Simulation-2: In this simulation, we examine the modulo

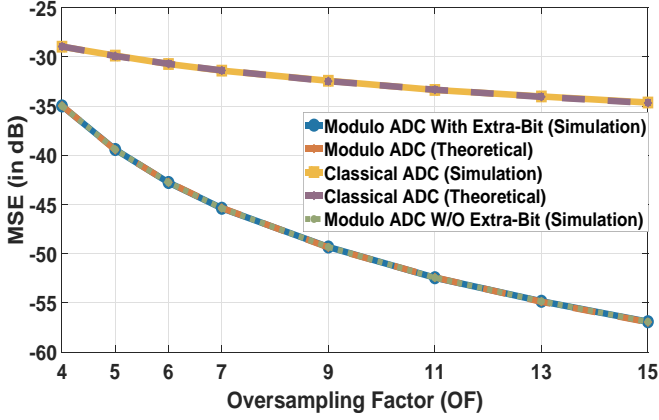


Fig. 5. Numerical and theoretical MSE results vs. OF for modulo ADC with and without extra 1-bit side information, and conventional ADC.

ADC system without the additional 1-bit side information. Specifically, we analyze the MSE variation, as detailed in Theorem 3 and (7), across different OF values. The input signal settings align with those of Simulation-1, featuring $b = 4$, OF ranging from 4 to 15, an OMP stopping criteria parameter of $\eta = 0.8$, and 20000 i.i.d noise realizations. Fig. 5 shows the variation of MSE, between true samples and estimated samples, for this setting as OF varies. The figure clearly demonstrates that modulo ADCs with and without extra-bit side information exhibit superior quantization noise suppression compared to the conventional ADC. Furthermore, our theoretical predictions align well with the simulated results; highlighting that the MSE diminishes at rates of $\mathcal{O}\left(\frac{1}{\text{OF}^3}\right)$ and $\mathcal{O}\left(\frac{1}{\text{OF}}\right)$ for the modulo ADC and conventional ADC, respectively.

Simulation-3: In this simulation, we analyze modulo ADC systems with and without additional 1-bit information, as well as conventional ADCs, to capture both weak and strong signals occupying distinct frequency bands. Specifically, we validate the upper bound on the NMSE for varying OF values, as stated in Corollary 1 and (15), for both strong and weak signal components. The analysis employs the BL signal model described in (13), with parameters $\alpha_1 = 1$ and $\alpha_2 = 0.25$. The signals $f_1(t)$ and $f_2(t)$ are synthesized using the $\text{sinc}(\cdot)$ function, where the bandwidth of $f_1(t)$ is $[-20 \text{ Hz}, 20 \text{ Hz}]$, and the bandwidth of $f_2(t)$ is $[-90 \text{ Hz}, -50 \text{ Hz}] \cup [50 \text{ Hz}, 90 \text{ Hz}]$. The simulation parameters are configured as follows: $b = 4$, OF ranging from 4 to 11, an OMP stopping criteria parameter of $\eta = 0.7$, and 5000 i.i.d noise realizations. Fig. 6 and Fig. 7 illustrate the variation in NMSE across different OF values for recovering the strong and weak signal components, respectively. These results demonstrate that the modulo ADC outperforms the conventional ADC in simultaneous acquisition of both strong and weak amplitude components that occupy different frequency bands in a BL signal. Furthermore, these simulation results validate the proposed theoretical upper bound on NMSE. Therefore, the NMSE decreases at rates of $\mathcal{O}\left(\frac{1}{\text{OF}^3}\right)$ and $\mathcal{O}\left(\frac{1}{\text{OF}}\right)$ for the modulo ADC and conventional ADC, respectively, during the acquisition of strong and weak signal components in a BL signal.

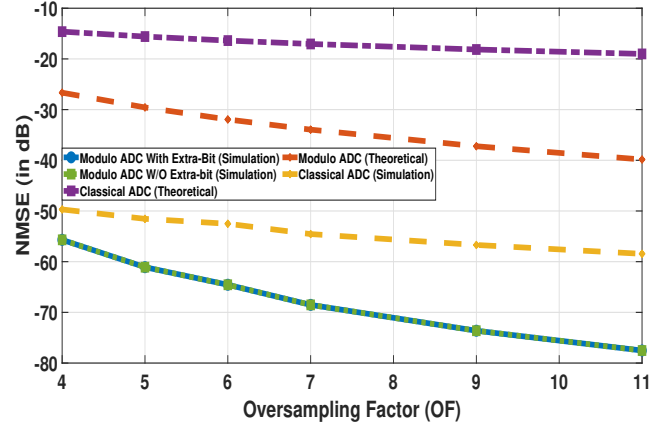


Fig. 6. Numerical and theoretical NMSE vs. OF for modulo ADC (with/without extra 1-bit information) and conventional ADC in recovering the strong signal component of a BL signal.

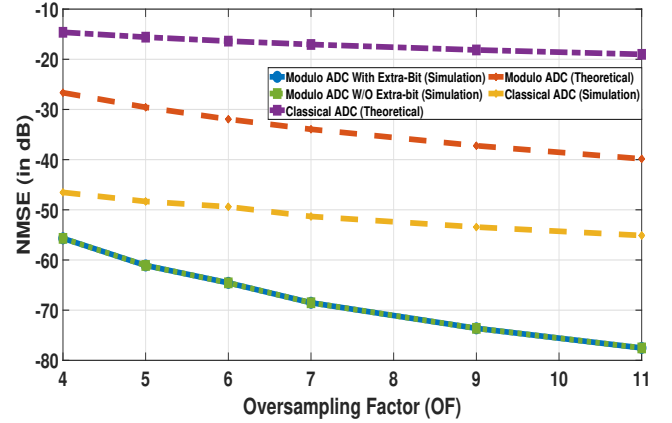


Fig. 7. Numerical and theoretical NMSE vs. OF for modulo ADC (with/without extra 1-bit information) and conventional ADC in recovering the weak signal component of a BL signal.

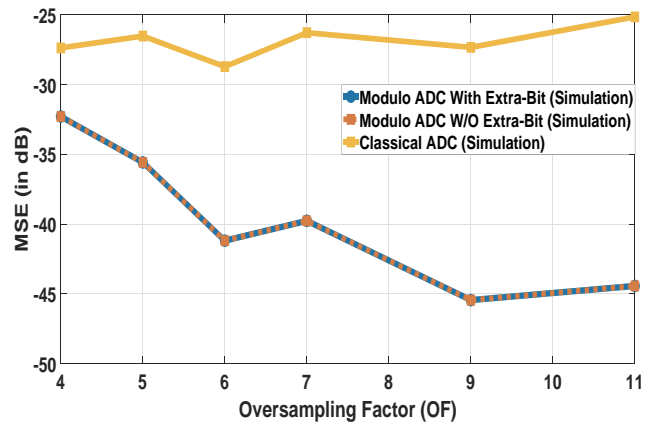


Fig. 8. Numerical MSE vs. OF result for modulo ADC (with) with and without extra 1-bit side information, and conventional ADC.

Simulation-4: Both previous simulations use the dither quantization framework. Here, we demonstrate that even without a dither signal (i.e., using the conventional quantization framework), the modulo ADC combined with the proposed recovery algorithms outperforms the classical ADC. For this

analysis, we consider an input signal with the same settings as Simulation-1: $b = 4$, an oversampling factor (OF) ranging from 4 to 11, an OMP stopping criterion parameter of $\eta = 0.8$, a modulo threshold $\lambda = \frac{1}{\text{OF}-2}$, and 5000 i.i.d. noise realizations. Fig. 8 illustrates the variation in MSE across different OF values for both modulo and classical ADCs. The results show that the modulo ADC, with or without 1-bit information, consistently outperforms the classical ADC.

VI. SUMMARY

This study analyzed the performance of a modulo ADC in the presence of a dithered quantization framework. We first considered the modulo ADC with 1-bit folding information and presented a recovery algorithm to unfold the modulo ADC samples. By using a dithered quantization framework for analysis, we showed that $\text{OF} > 3$ and $b > 3$ are sufficient conditions for the modulo ADC with 1-bit folding information to achieve better quantization noise suppression when compared to a conventional ADC with the same number of bits used for amplitude quantization. Moreover, the MSE of modulo ADC decays faster than that of conventional ADC as OF is increased. When the 1-bit folding information is not available, we showed that OMP can be incorporated in the recovery algorithm to obtain the same MSE performance. However, the sufficient condition on the number of quantization bits is increased. We also analyzed the case of simultaneous acquisition of weak and strong signals occupying different frequency bands and demonstrated the superior performance of modulo ADC over conventional ADC. Numerical results are provided to substantiate the performance guarantees derived in this work.

APPENDIX A PROOF OF LEMMA 1

A necessary condition for \mathbf{V}_S to be full column rank is $|\mathcal{S}| \leq K$. Since the columns of \mathbf{V}_S are from the columns of the Fourier basis, they are linearly independent. Thus, the condition $|\mathcal{S}| \leq K$ is also sufficient.

We first provide an upper bound for $|\mathcal{S}|$. Using [15, Equation 7], we have

$$\begin{aligned} |\mathcal{S}| &\leq 4 \left\lfloor \frac{\rho N}{2} \right\rfloor + 4 \left\lfloor \frac{\rho N}{2} \right\rfloor \cdot \left\lfloor \frac{\|f(t)\|_\infty - \lambda'}{2\lambda'} \right\rfloor \\ &\leq 2\rho N + 2\rho N \cdot \left(\frac{\|f(t)\|_\infty - \lambda'}{2\lambda'} \right), \end{aligned} \quad (17)$$

where the second inequality comes from the trival upper bound of the floor function, i.e., $\lfloor x \rfloor \leq x$. Meanwhile, $K = N - 2 \lfloor \frac{\rho N}{2} \rfloor \geq (1 - \rho)N$. Hence, for \mathbf{V}_S to be a full column rank matrix, it suffices to show that

$$2\rho N + 2\rho N \cdot \left(\frac{\|f(t)\|_\infty - \lambda'}{2\lambda'} \right) \leq (1 - \rho)N.$$

After some algebraic manipulation, we get

$$\lambda' \geq \frac{\rho}{1 - 2\rho} \|f(t)\|_\infty \quad \left(\text{or } \lambda' \geq \frac{\|f(t)\|_\infty}{\text{OF} - 2} \right). \quad (18)$$

Since $\lambda' < \|f(t)\|_\infty$, there exists a λ' that satisfies the above inequality when $\rho < \frac{1}{3}$, i.e., $\text{OF} > 3$.

APPENDIX B PROOF OF THEOREM 1

We first bound the ℓ_∞ -norm of the estimate of first-order difference of the modulo residue:

$$\begin{aligned} \|\Delta \hat{\mathbf{z}} - \Delta \mathbf{z}\|_\infty &= \|\mathbf{V}_S^\dagger \mathbf{y} - \Delta \mathbf{z}_S\|_\infty \\ &= \|\mathbf{V}_S^\dagger \mathbf{V}_S (\Delta \mathbf{z}_S + \Delta \epsilon_S) - \Delta \mathbf{z}_S\|_\infty \\ &= \|\Delta \epsilon_S\|_\infty \\ &\leq \frac{6\lambda}{2^b} \\ &= \frac{6\lambda'}{2^b - 2}, \end{aligned}$$

where $\Delta \epsilon_S$ contains the values of $\Delta \epsilon[n]$ at the indices contained in \mathcal{S} . The third line follows because \mathbf{V}_S is full column rank by Lemma 1. The fourth line holds because $\epsilon[n]$ induced by the triangle dither $d[n]$ has amplitude support $(-\frac{3\lambda}{2^b}, +\frac{3\lambda}{2^b})$. Hence, $|\Delta \epsilon[n]| \leq \frac{6\lambda}{2^b}$ for all n .

To ensure that we perfectly recover the modulo residue after the rounding operation, we must have

$$\frac{6\lambda'}{2^b - 2} < \lambda' \implies b > 3, \quad (19)$$

which is an explicit assumption of the theorem. Under this setting, $z[n] - \hat{z}[n] = 0$. Consequently, from (5), the MSE becomes

$$\begin{aligned} \text{MSE} &= \mathbb{E} \left[(\text{LPF}\{\epsilon[n]\})^2 \right] \\ &= \rho \frac{\lambda^2}{2^{2b}} \\ &= \frac{\lambda'^2}{\text{OF}(2^b - 2)^2}. \end{aligned} \quad (20)$$

Since the MSE grows quadratically with λ' , we should set the value of λ' as low as possible. Noting that λ' should satisfy (18), we obtain the desired result by setting $\lambda' = \frac{\|f(t)\|_\infty}{\text{OF} - 2}$.

APPENDIX C PROOF OF THEOREM 3

Recall that finding the unknown support \mathcal{S} of $\Delta z[n]$ is the same as finding $c[n]$. We focus on the former. Since the nonzero elements of the modulo residue have amplitudes $(2\mathbb{Z} + 1)\lambda'$, we get

$$\min_{n \in \mathcal{S}} |\Delta z[n]| = \lambda'.$$

In addition,

$$\begin{aligned} \|\mathbf{V}^H \mathbf{V} \Delta \epsilon\|_\infty &\leq \|\mathbf{V}^H \mathbf{V}\|_\infty \|\Delta \epsilon\|_\infty \\ &\leq \eta \frac{6\lambda'}{2^b - 2} \end{aligned}$$

By Theorem 2, exact support recovery is guaranteed if

$$\begin{aligned} \lambda' &> \frac{(\sqrt{1 + \delta_{L_0+1}} + 1) \sqrt{L_0}}{1 - (\sqrt{L_0} + 1) \delta_{L_0+1}} \left(\eta \frac{6\lambda'}{2^b - 2} \right) \\ \implies b &> \log_2 \left\{ 6\eta \cdot \frac{(\sqrt{1 + \delta_{L_0+1}} + 1) \sqrt{L_0}}{1 - (\sqrt{L_0} + 1) \delta_{L_0+1}} + 2 \right\} \\ &= 3 + \log_2 \left\{ \frac{3\eta \cdot \frac{(\sqrt{1 + \delta_{L_0+1}} + 1) \sqrt{L_0}}{1 - (\sqrt{L_0} + 1) \delta_{L_0+1}} + 1}{4} \right\}. \end{aligned}$$

With support \mathcal{S} perfectly recovered, the signal recovery block effectively has the 1-bit folding information signal $c[n]$. The proof is completed by applying the theoretical guarantees in Theorem 1.

APPENDIX D
PROOF OF COROLLARY 1

From Theorem 1, $z[n] - \hat{z}[n] = 0$ if $b > 3$ and $\text{OF} > 3$. The normalized MSE of recovering the i -th component becomes

$$\begin{aligned} \frac{\mathbb{E}[(\alpha_i f_i[n] - \hat{f}_i[n])^2]}{\mathbb{E}[(\alpha_i f_i[n])^2]} &= \frac{1}{\alpha_i^2} \mathbb{E}[(\text{BPF}_i\{\epsilon[n]\})^2] \\ &= \frac{\rho}{\alpha_i^2} \cdot \frac{\omega_i}{\omega_m} \cdot \frac{2\lambda'^2}{(2^b - 2)^2}. \end{aligned} \quad (21)$$

Setting λ' to be the RHS of (18) and replacing $\|f(t)\|_\infty$ by its upper bound $\sqrt{\frac{\omega_m(\alpha_1^2 + \alpha_2^2)}{\pi}}$ complete the proof.

REFERENCES

- [1] Y. C. Eldar, *Sampling Theory: Beyond Bandlimited Systems*. Cambridge University Press, 2015.
- [2] P. E. Debevec and J. Malik, "Recovering High Dynamic Range Radiance Maps from Photographs," in *ACM Siggraph*, 1997, p. 369–378.
- [3] K. Yamada, T. Nakano, and S. Yamamoto, "A vision sensor having an expanded dynamic range for autonomous vehicles," *IEEE Trans. Veh. Technol.*, vol. 47, no. 1, pp. 332–341, 1998.
- [4] J. Zhang, J. Hao, X. Zhao, S. Wang, L. Zhao, W. Wang, and Z. Yao, "Restoration of clipped seismic waveforms using projection onto convex sets method," *Nature Sci. Rep.*, vol. 6, no. 39056, 2016.
- [5] B. F. Logan, "Signals designed for recovery after clipping — ii. fourier transform theory of recovery," *AT&T Bell Laboratories Technical Journal*, vol. 63, no. 2, pp. 287–306, 1984.
- [6] J. Abel and J. Smith, "Restoring a clipped signal," in *[Proceedings] ICASSP 91: 1991 International Conference on Acoustics, Speech, and Signal Processing*, 1991, pp. 1745–1748 vol.3.
- [7] S.-K. Ting and A. H. Sayed, "Mitigation of clipping in sensors," in *2013 IEEE International Conference on Acoustics, Speech and Signal Processing*, 2013, pp. 5934–5938.
- [8] F. Esqueda, S. Bilbao, and V. Välimäki, "Aliasing reduction in clipped signals," *IEEE Transactions on Signal Processing*, vol. 64, no. 20, pp. 5255–5267, 2016.
- [9] A. Bhandari, F. Kraher, and R. Raskar, "On unlimited sampling and reconstruction," *IEEE Transactions on Signal Processing*, vol. 69, pp. 3827–3839, 2021.
- [10] E. Romanov and O. Ordentlich, "Above the Nyquist Rate, Modulo Folding Does Not Hurt," *IEEE Signal Process. Lett.*, vol. 26, no. 8, pp. 1167–1171, 2019.
- [11] S. Rudresh, A. Adiga, B. A. Shenoy, and C. S. Seelamantula, "Wavelet-based reconstruction for unlimited sampling," in *2018 IEEE International Conference on Acoustics, Speech and Signal Processing (ICASSP)*, 2018, pp. 4584–4588.
- [12] A. Bhandari, F. Kraher, and T. Poskitt, "Unlimited Sampling From Theory to Practice: Fourier-Prony Recovery and Prototype ADC," *IEEE Trans. Signal Process.*, vol. 70, pp. 1131–1141, 2022.
- [13] E. Azar, S. Mulleti, and Y. C. Eldar, "Residual Recovery Algorithm for Modulo Sampling," in *Proc. IEEE Int. Conf. Acoust., Speech, Signal Process.*, 2022, pp. 5722–5726.
- [14] —, "Unlimited sampling beyond modulo," *Applied and Computational Harmonic Analysis*, vol. 74, p. 101715, 2025. [Online]. Available: <https://www.sciencedirect.com/science/article/pii/S1063520324000927>
- [15] S. B. Shah, S. Mulleti, and Y. C. Eldar, "Lasso-based fast residual recovery for modulo sampling," in *ICASSP 2023 - 2023 IEEE International Conference on Acoustics, Speech and Signal Processing (ICASSP)*, 2023, pp. 1–5.
- [16] —, "Compressed sensing based residual recovery algorithms and hardware for modulo sampling," *arXiv preprint arXiv:2412.12724*, 2024. [Online]. Available: <https://arxiv.org/abs/2412.12724>
- [17] S. Mulleti, E. Reznitskiy, S. Savariego, M. Namer, N. Glazer, and Y. C. Eldar, "A hardware prototype of wideband high-dynamic range analog-to-digital converter," *IET Circuits, Devices & Systems*, vol. 17, no. 4, pp. 181–192, 2023.
- [18] S. Mulleti, A. Eyar, S. B. Shah, N. Glazer, S. Savariego, O. Cohen, E. Reznitskiy, M. Namer, and Y. C. Eldar, "Hardware demonstration of low-rate and high-dynamic range ADC," *Show and Tell Demos, IEEE International Conference on Acoustics, Speech and Signal Processing (ICASSP)*, 2022.
- [19] Y. Kvich, S. Savariego, M. Namer, and Y. C. Eldar, "Practical modulo sampling: Mitigating high-frequency components," (*manuscript under preparation*), 2024.
- [20] A. Bhandari, "Back in the us-sr: Unlimited sampling and sparse super-resolution with its hardware validation," *IEEE Signal Processing Letters*, vol. 29, pp. 1047–1051, 2022.
- [21] S. Mulleti and Y. C. Eldar, "Modulo sampling of FRI signals," *IEEE Access*, vol. 12, pp. 60 369–60 384, 2024.
- [22] O. Musa, P. Jung, and N. Goertz, "Generalized approximate message passing for unlimited sampling of sparse signals," in *2018 IEEE Global Conference on Signal and Information Processing (GlobalSIP)*, 2018, pp. 336–340.
- [23] D. Prasanna, C. Sriram, and C. R. Murthy, "On the identifiability of sparse vectors from modulo compressed sensing measurements," *IEEE Signal Processing Letters*, vol. 28, pp. 131–134, 2021.
- [24] V. Shah and C. Hegde, "Sparse signal recovery from modulo observations," *EURASIP Journal on Advances in Signal Processing*, vol. 2021, no. 1, pp. 1–17, 2021.
- [25] F. Ji, Pratibha, and W. P. Tay, "Unlimited dynamic range signal recovery for folded graph signals," *Signal Processing*, vol. 198, p. 108574, 2022. [Online]. Available: <https://www.sciencedirect.com/science/article/pii/S0165168422001177>
- [26] Y. Kvich and Y. C. Eldar, "Modulo sampling and recovery in shift-invariant spaces," in *ICASSP 2024 - 2024 IEEE International Conference on Acoustics, Speech and Signal Processing (ICASSP)*, 2024, pp. 11–15.
- [27] —, "Modulo sampling in shift-invariant spaces: Recovery and stability enhancement," 2024. [Online]. Available: <https://arxiv.org/abs/2406.10929>
- [28] T. Feuillen, B. Shankar MRR, and A. Bhandari, "Unlimited sampling radar: Life below the quantization noise," in *ICASSP 2023 - 2023 IEEE International Conference on Acoustics, Speech and Signal Processing (ICASSP)*, 2023, pp. 1–5.
- [29] A. Krishna, S. Rudresh, V. Shaw, H. R. Sabbella, C. S. Seelamantula, and C. S. Thakur, "Unlimited dynamic range analog-to-digital conversion," 2019.
- [30] L. Schuchman, "Dither signals and their effect on quantization noise," *IEEE Transactions on Communication Technology*, vol. 12, no. 4, pp. 162–165, 1964.
- [31] R. Gray and T. Stockham, "Dithered quantizers," *IEEE Transactions on Information Theory*, vol. 39, no. 3, pp. 805–812, 1993.
- [32] N. I. Bernardo, S. B. Shah, and Y. C. Eldar, "Modulo sampling with 1-bit side information: Performance guarantees in the presence of quantization," in *2024 IEEE International Symposium on Information Theory (ISIT)*, 2024, pp. 3498–3503.
- [33] I. S. Gradshteyn and I. M. Ryzhik, *Table of integrals, series, and products*, 7th ed. Elsevier/Academic Press, Amsterdam, 2007, translated from the Russian, Translation edited and with a preface by Alan Jeffrey and Daniel Zwillinger, With one CD-ROM (Windows, Macintosh and UNIX).
- [34] S. Mallat and Z. Zhang, "Matching pursuits with time-frequency dictionaries," *IEEE Transactions on Signal Processing*, vol. 41, no. 12, pp. 3397–3415, 1993.
- [35] Y. C. Eldar and G. Kutyniok, *Compressed sensing: theory and applications*. Cambridge University Press, 2012.
- [36] T. T. Cai and L. Wang, "Orthogonal matching pursuit for sparse signal recovery with noise," *IEEE Transactions on Information Theory*, vol. 57, no. 7, pp. 4680–4688, 2011.
- [37] R. Wu, W. Huang, and D.-R. Chen, "The exact support recovery of sparse signals with noise via orthogonal matching pursuit," *IEEE Signal Processing Letters*, vol. 20, no. 4, pp. 403–406, 2013.
- [38] A. S. Bandeira, E. Dobriban, D. G. Mixon, and W. F. Sawin, "Certifying the restricted isometry property is hard," *IEEE Transactions on Information Theory*, vol. 59, no. 6, pp. 3448–3450, 2013.
- [39] A. Papoulis, "Limits on bandlimited signals," *Proceedings of the IEEE*, vol. 55, no. 10, pp. 1677–1686, 1967.
- [40] F. Harris, *Multirate Signal Processing for Communication Systems*, ser. River Publishers Series in Signal, Image and Speech Processing. River Publishers, 2021.